CRYSTAL GROWTH & DESIGN
2004
VOL. 4, NO. 2
331−335

Controlled Deposition of Thin Films of Calcium Carbonate on Natural and Synthetic Templates

Parayil Kumaran Ajikumar,[†] Rajamani Lakshminarayanan,[‡] and Suresh Valiyaveettil*[,†,‡]

Singapore-MIT Alliance, Department of Chemistry, National University of Singapore, Singapore, 117 543

Received July 12, 2003; Revised Manuscript Received November 11, 2003

ABSTRACT: Thin films of calcium carbonate polymorphs were grown on natural and synthetic scaffolds in the presence of acidic polymers. Decalcified eggshell membrane and Nylon 66 fiber knits were used as 3D scaffolds, and acidic polymers such as polyaspartic acid, polyglutamic acid, and poly(acrylic acid) were used as control macromolecules. The Nylon 66 knits preadsorbed with acidic polymers produced thin films of calcite phase, whereas smooth vaterite or aragonite thin films were formed on the eggshell membrane. The preadsorption of the soluble macromolecules was characterized by the ATR-FTIR spectroscopy. The characterization of the mineral films was carried out using scanning electron microscope, X-ray diffraction, and energy-dispersive X-ray scattering investigations.

Introduction

Synthesis of thin film coatings of organic−inorganic hybrid materials have been explored extensively owing to their potential for biomedical and industrial applications.[1−5] The fabrication of such composite materials with a control over the shape and properties can be achieved by adopting the natural process of matrix-mediated biomineralization.[6−8] In biological environments, this process is controlled or facilitated by biomacromolecules such as proteins and proteoglycans.[9−14] Such mineral phases are produced under strict biogenic control through an interplay of templating and inhibition mechanism between the "unusually" acidic water soluble proteins and highly hydrophobic biomacromolecules. The hydrophobic biomacromolecules function as a three-dimensional scaffold, whereas the acidic biomacromolecules act as a control in the deposition of minerals. The resultant mineral phase is highly oriented and possesses interesting mechanical properties as compared to the one produced in the laboratory.[15,16] Numerous methods have been used to study the controlled mineral formation using synthetic templates.[17−31]

For calcium carbonate thin film development, the most commonly used insoluble matrixes were chitin, chitosan, and cellulose, which contains functional groups such as -OH, >C═O, and -NH- moieties.[20,22,35] Recently, Kato et al. demonstrated polymorph selectivity in $CaCO_3$ thin film deposition using synthetic macromolecules.[32] In our earlier work, we have shown that poly(vinyl alcohol) (PVA) adsorbed polyamide fibers induced the selective nucleation of calcium carbonate polymorphs.[33,34] Here we focus on the deposition of thin films of calcium carbonate polymorphs on biocompatible matrixes such as Nylon 66 fiber knit and demineralized eggshell membrane scaffolds with different surface morphologies (Figure 1A,B). Nylon is a biocompatible polymer with potential applications in the biomedical industry and is extensively used as a tissue engineering scaffold for the growth of tissues, tissue interfaces, and blood vessels.[35−37] We chose Nylon 66 knits as a scaffold for calcium carbonate coating because of its structural similarity with the polyalanine/polyglycine domains in the insoluble matrix proteins from the prismatic nacreous layer.[38] The avian eggshell is a biomineralized composite consisting of calcium carbonate embedded in an organic matrix.[39] The second scaffold, the semipermeable eggshell membrane, is a naturally occurring collagenous organic matrix that is associated with calcium carbonate biominerals and can be used for the development of biocompatible hybrid materials and templates.[40] The outer part of the eggshell membrane consists of fibrillar collagens (type I, V, and X) and glycosaminoglycans, all of which act as templates for the calcium carbonate crystallization.[41] The SEM of the demineralized eggshell membrane showed the presence of interwoven network of collagen fibrils (Figure 1B). In addition to this, establishing the role of the amide, amine, and the carboxylic acid groups present on the surface of the Nylon 66 knits and the eggshell membrane toward $CaCO_3$ thin film deposition is an interesting challenge. Acidic polymers such as polyaspartic acid (PAsp), polyglutamic acid (PGlu), and poly(acrylic acid) (PA) were preadsorbed on the Nylon 66 fiber knits and eggshell membrane to control the morphology and polymorph selectivity. In brief, the present paper delineates the preparation of biocompatible calcium car-

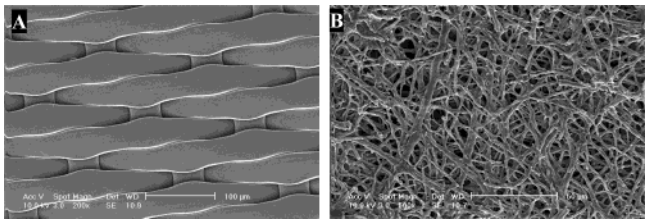

Figure 1. SEM images of the surface morphology of Nylon 66 knit (A) and demineralized eggshell membrane (B).

* Corresponding author. E-mail: chmsv@nus.edu.sg. Tel: (65)-8744327. Fax: (65)7791691.
[†] Singapore-MIT Alliance.
[‡] Department of Chemistry, National University of Singapore.

10.1021/cg034128e CCC: $27.50
Published on Web 12/20/2003

bonate coatings by the judicious choice of the templates and water soluble additives.

Experimental Procedures

PAsp (Mw 8300) and PGlu (Mw 5800) were purchased from Sigma and PA (Mw 5000) was from Aldrich Chemical Company. The Nylon 66 fiber knit was supplied by SEFAR Singapore Pvt Ltd. Water was purified by Mill-RO plus system (Millipore) and used in all experiments. The eggshell membrane was prepared from the commercially available fresh chicken eggshells. The eggshells were thoroughly washed with Millipore water, decalcified with 1 N HCl for 30 min, and the eggshell membrane was collected and washed with water.

The Nylon 66 fiber knits and eggshell membranes were cut into small pieces (1 × 1 cm). $CaCO_3$ crystals were grown from a supersaturated calcium bicarbonate ($Ca(HCO_3)_2$) solution, which was prepared by passing carbon dioxide (CO_2) gas for 5 h to a stirred suspension of calcium carbonate in water. The undissolved calcium carbonate was removed by filtration and CO_2 gas was passed through the resulting clear solution for 1 h to dissolve any residual nuclei formed. The Ca^{2+} ion concentration in solution was calculated using elemental analysis (7.2−7.5 mmol/L). The pH of the freshly prepared solution was measured and found to be at a value of 5.9−6.1. The crystals were grown using a small crystallization dish for a period of 96 h, unless specified otherwise.

For acid and alkali treatments, the fiber knits were treated with dilute hydrochloric acid or sodium hydroxide (1.5 N) solutions for 24 h at room temperature. The preadsorption of the acidic polymers on the fiber knit and eggshell membrane surface was done by soaking pieces of the samples in the appropriate polymer solution (1 mL) with a concentration of 5% (w/v) for 24 h. The fiber knits were removed and rinsed thoroughly with water 4−5 times, and the excess water was blotted. Crystals were grown on the surface using the procedure reported elsewhere.[42]

Powder X-ray diffraction studies on the crystals collected were done using a D5005 Siemens X-ray diffractometer with Cu Kα radiation at 40 kV and 40 mA. The crystals grown on the fiber knit were mounted on a plastic holder and diffraction studies were carried out. The phase identification was done by comparing the peak positions in the X-ray diffraction data of the crystals with the standard data available from Joint Committee on Powder Diffraction Standards.

Morphological studies were carried out using a Philips XL-30 scanning electron microscope (SEM). The samples were carefully mounted on copper stubs with a double-sided carbon tape and then sputter coated with gold before examination. Energy-dispersive X-ray analyses were performed at various locations on the substrate to confirm the presence of $CaCO_3$ crystals or film. The ATR-FTIR spectra were collected on a Seagull attachment to the Perkin-Elmer Spectrum 2000 spectrophotometer equipped with a N_2 gas generator and a DTG detector, with Nylon 66 fiber knits and eggshell membranes mounted on a ZnSe crystal (45° angle of incidence). 32 scans were collected and averaged at a resolution of 4 cm^{-1}.

Results

Preparation and Characterization of the Surface-Modified Scaffolds. The treated or untreated fiber knits were preadsorbed with water-soluble acidic polymers as described in the experimental section. To understand the surface modifications due to the acid or alkali treatments, the surface of the fiber knits were characterized using ATR-FTIR spectroscopy. The spectra of the untreated fiber knit showed characteristic N−H and >C═O stretching vibrations at 3300 and 1630 cm^{-1}, respectively, which correspond to the hydrogen bonded Nylon 66 chains. Figure 2A shows the ATR-FTIR spectra of untreated and acid-/alkali-treated Nylon 66 knits. A significant increase in the intensity and broadening of the -NH stretching band was observed after acid or alkali treatment. The ratio of the calculated peak area under the -NH region is ca. 1:3:2 and for the >C═O region is ca. 1:2:2 for untreated, acid-treated, and alkali-treated Nylon 66 fiber knits, respectively. The increase in the peak area demonstrates the microenvironmental changes on the fiber surface. Preadsorption of acidic polypeptides (e.g., PAsp and PGlu) on the fiber surface resulted in approximately a 4-fold increase in the peak area (A) (i.e., for the -NH peak, $A_{unadsorbed}/A_{PAsp}/A_{PGlu}$ = 1:5:4 and for the >C═O peak, $A_{unadsorbed}/A_{PAsp}/A_{PGlu}$ = 1:4:4, Figure 2B). In all the above cases, the peak area obtained from the untreated or unadsorbed fiber knit surfaces was chosen as the standard for comparison. Interestingly, the preadsorption of PA resulted in the decrease of -NH and >C═O peak intensity. Moreover, the appearance of a peak at 1720 cm^{-1} confirmed the presence of PA on the fiber surface (Figure 2B). In the case of the eggshell membrane, characterization of the changes in PAsp and PGlu adsorbed surfaces was complicated by the appearance of broad absorption peaks, especially in the region of the 2900−3600 cm^{-1} range (Figure 3). However, there are remarkable changes in the IR spectra of the PA preadsorbed eggshell membrane with an appearance of a shoulder peak at 1705 cm^{-1} with a broadening of the amide peak at 1630 cm^{-1}.

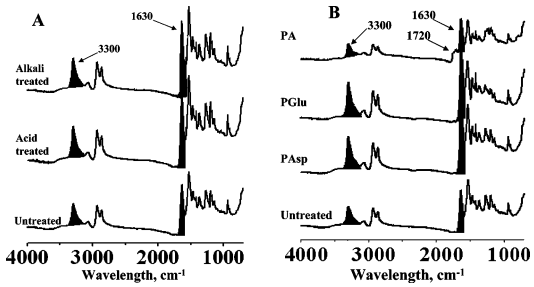

Figure 2. ATR-FTIR spectra (absorbance mode) of the Nylon 66 fiber knit (A). The strong band around 3300 cm^{-1} is assigned to -NH stretching. Nylon 66 fiber knit after preadsorption of soluble acidic polymers (B). The amide band observed at 1630 cm^{-1} showed an enhancement in intensity in the presence of the polypeptides.

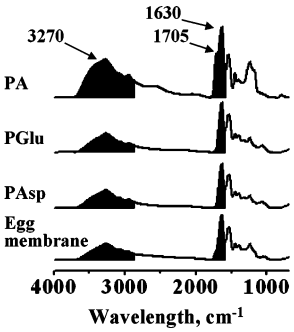

Figure 3. ATR-FTIR spectra (absorbance mode) of the eggshell membrane before and after preadsorption of the soluble acidic polymers. The broad band around 3270 cm^{-1} is assigned to amide -NH and carboxylic -OH stretching before and after treatments. The amide bands observed at 1630 cm^{-1} showed an enhancement in intensity in the presence of the polypeptides.

Thin Film Deposition of Calcium Carbonate. The crystallization experiments were performed by soaking

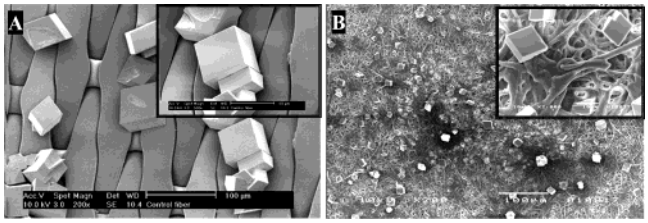

Figure 4. SEM image of the calcite crystals on untreated Nylon 66 knit (A) and eggshell membrane (B).

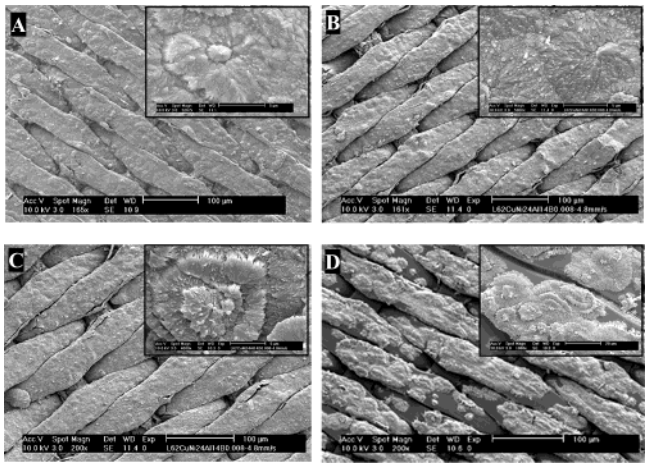

Figure 5. Representative SEM image of the thin film calcite crystals on untreated (A), acid-treated (B), and alkali-treated (C) Nylon 66 knit preadsorbed with PAsp, after 96 h. The thin film growth over the PAsp preadsorbed untreated fiber knit after 48 h (D). The magnified images are given in the inset.

Table 1. Details of the Various $CaCO_3$ Crystallization Experiments Performed on Nylon 66 Fiber Knit and Demineralized Eggshell Membrane Scaffolds

	acidic polymer adsorbed		
scaffold	PAsp	PGlu	PA
Nylon 66 knit	calcite film	calcite crystals	calcite crystals
eggshell membrane	vaterite film	aragonite film	no coating

the untreated or chemically modified Nylon 66 knit into a supersaturated solution of calcium bicarbonate for 96 h at 25 °C.

The morphology and nature of the minerals grown on the scaffolds were examined using a scanning electron microscope (SEM) and X-ray diffraction method. The results are summarized in Table 1.

Calcite rhombohedral crystals were observed in the case of the untreated or treated Nylon 66 knits and eggshell membrane after crystallization for 96 h (Figure 4). However, a thin film was deposited on all fiber knit surfaces preadsorbed with PAsp (Figure 5A−C). From the SEM of crystals deposited after 48 h, it appears that the spherical microcrystallites are nucleated first and gradually spread over the whole functionalized surface. XRD patterns confirmed the presence of the calcite phase, and the appearance of diffraction peaks from all crystal planes of the calcite lattice indicates the lack of any preferential orientation (Figure 6). The presence of Ca on the scaffold surface was further confirmed by the EDX analysis. In the case of the PA preadsorbed fiber knit, there was no contiguous thin film formation, and incomplete patches of calcite crystals were deposited over the fiber knit (Figure 7A). PGlu preadsorbed

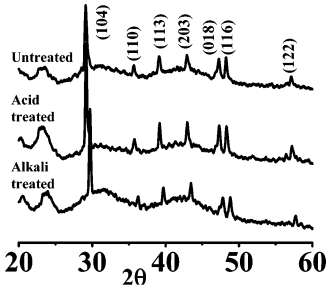

Figure 6. XRD patterns of the thin films of calcite on Nylon 66 fiber knit preadsorbed with PAsp.

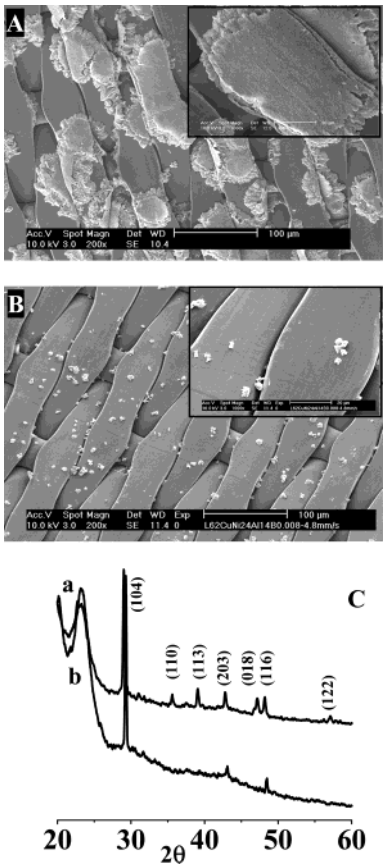

Figure 7. SEM images of calcite crystals on PA (A) and PGlu (B) preadsorbed Nylon 66 fiber knit. The magnified images are given in the inset. XRD patterns (C) of the crystals deposited on PA (a) and PGlu (b) preadsorbed Nylon 66 fiber knit indicate sharp diffraction peaks for calcite phase.

surface induced the nucleation of small calcite crystal islands (Figure 7B). Here also the nature of the polymorph was identified as calcite using the X-ray diffraction pattern (Figure 7C). In the case of the eggshell membrane, a complete surface coverage of the mineral layer was observed in the presence of PAsp (Figure 8A). The mineral phase was identified as vaterite using powder X-ray diffraction pattern as given in Figure 8C. However, in the presence of PGlu, a smooth thin film of aragonite phase was observed (Figure 8B,D). In both cases, EDX analyses confirmed the presence of the $CaCO_3$ thin films on the surface of the eggshell membrane. Membrane preadsorbed with PA strongly suppressed the growth of calcium carbonate crystals (Figure 9).

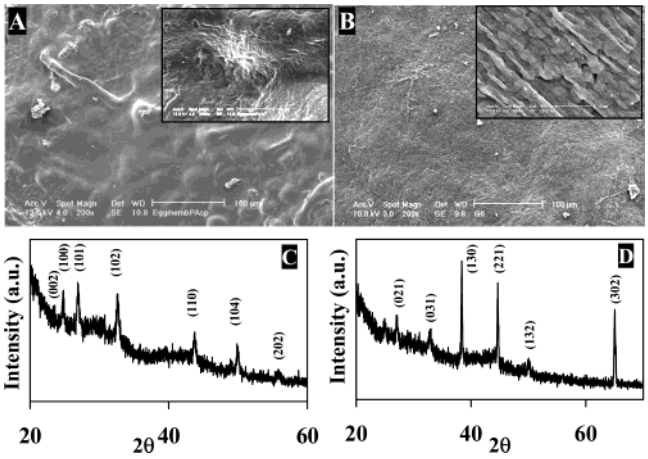

Figure 8. SEM image of the mineral film formed on PAsp (A) and PGlu (B) preadsorbed eggshell membrane. The magnified images are given in the inset. XRD of the thin film of $CaCO_3$ indicates sharp diffraction for the vaterite phase on PAsp preadsorbed eggshell membrane (C); XRD of the thin film on PGlu preadsorbed eggshell membrane indicates sharp diffraction for the aragonite phase (D).

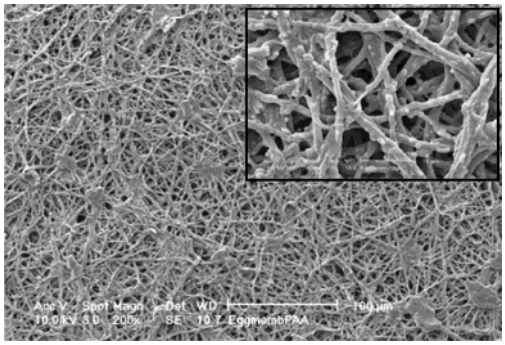

Figure 9. SEM micrographs of PA preadsorbed eggshell membrane after the crystal growth.

Discussion

The most commonly used insoluble natural matrixes for the deposition of thin films of different polymorphs of $CaCO_3$ were chitin, chitosan, and cellulose, which contains surface functional groups such as -OH, >C═O, and -NH-, and water-soluble polymer additives such as PAsp, PGlu, and PA with -COOH functional moieties.[42−44] In an earlier report, Gower et al. investigated the role of polypeptides in the deposition of calcium carbonate thin films through a polymer-induced liquid-precursor (PILP) process.[45] The polypeptide induces liquid−liquid-phase separation of droplets of precursor minerals followed by a deposition on the substrate and coalesce to form a coating, which then solidifies into thin films.

Using a similar approach, a few soluble macromolecules were preadsorbed to the polyamide fiber knit (untreated or treated) and eggshell membrane to induce the deposition of thin films of $CaCO_3$ polymorphs. ATR-FTIR data confirmed the adsorption of the acidic macromolecules on the surface of the scaffolds. The results are summarized in Table 1, which indicates the differences in nucleation and deposition of $CaCO_3$ crystals on synthetic or natural scaffolds in the presence of acidic polymers. Addadi et al. observed that PAsp exists as β-sheet conformation, whereas PGlu and PA exist as a random coil in calcium chloride solution.[46] Falini et al. reported that collagen bundles and oriented polypeptide chains have a significant role over the control of the polymorphism in calcium carbonate crystallization.[47] They reported a preferentially oriented and selective deposition of vaterite and aragonite in gelatin films containing a high concentration of polypeptides. The template Nylon 66 has an extended β-pleated sheet structure, whereas collagen contains helical bundles of proteinacious materials.[3,48] The PAsp preadsorbed Nylon knit nucleated the formation of a contiguous thin film, whereas the PGlu preadsorbed surfaces induced the deposition of small calcite crystal aggregates. In the case of the PA preadsorbed substrates, only patches of calcite thin films were observed. Thus, it is conceivable that the microenvironmental changes brought by the adsorption of acidic polypeptides play a significant role in inducing the deposition of thin films of calcium carbonate polymorphs. The eggshell membranes act as a template on which mineralization of the eggshell matrix occurs at a high rate in biogenic conditions.[49] During the eggshell mineralization, the calcium carbonate deposition begins on the outer side of the membranes and then progresses in an upward direction. However, the complex architecture of the calcified layer is a result of the interaction of calcium carbonate crystals with organic matrix molecules such as proteins and proteoglycans. In our in vitro experiments, rhombohedral calcite crystals were grown on the eggshell membrane without preadsorption of the acidic polymers. However, in the case of the PAsp preadsorbed eggshell membrane, a complete coating of a vaterite polymorph on the eggshell membrane was observed, whereas the PGlu preadsorbed membrane induced the nucleation of the aragonite phase. PA strongly suppressed crystal growth on the surface of the eggshell membrane scaffold. Addadi et al. reported that for the adsorption of the soluble polymers (PAsp, PGlu, and PA) over a sulfonated polystyrene film, both PAsp and PGlu adopted a β-sheet conformation, whereas the PA did not adopt an ordered conformation.[46] The crystal growth experiments performed on sulfonated polystyrene film showed that the PAsp and PGlu induced the nucleation of oriented calcite crystals, while PA did not induce the nucleation of calcite phase. In addition to this, the same PAsp adsorbed over the nonsulfonated polystyrene did not nucleate the calcite phase, indicating a cooperative effect of the functional groups on the surface of the insoluble template and the adsorbed soluble macromolecule in the calcium carbonate crystal nucleation. ATR-FTIR studies indicated both peptides adopted a β-sheet conformation on the eggshell membrane scaffold. Hence, the observed polymorph selectivity in the case of the modified eggshell membrane might be due to the combined effect of the preadsorbed macromolecules (PAsp and PGlu) and the surface functionalities on the scaffold. The geometrical matching between the position of the oriented functional group and the crystal plane may also play an important role. These results clearly show that microstructure of the preadsorbed surfaces has a significant control over the polymorphism and calcium carbonate crystallization over the modified egg membranes.

In conclusion, we investigated the deposition of thin films of calcium carbonate polymorphs on the Nylon 66

fiber knit and demineralized eggshell membrane. The surface modifications of the fiber knit were achieved either by the chemical treatment or by the preadsorption of acidic polymers. The PAsp preadsorbed Nylon 66 fiber knit surfaces favor the deposition of calcite thin films, whereas vaterite or aragonite mineral phases were deposited on the surface of PAsp or PGlu adsorbed eggshell membranes, respectively. The above-described biomimetic approach has implications toward understanding the combined role of template and acidic polymers in the biomineralization process and is believed to be the first example in which Nylon 66 knits and eggshell membranes were used as templates for the preparation of biocompatible calcium carbonate thin films. These biocompatible calcium carbonate coatings might be useful for tissue engineering applications and also for fundamental studies of cell−matrix interactions.

Acknowledgment. The authors thank the Singapore-MIT Alliance, Singapore, for financial support. We also acknowledge the technical support from the Department of Chemistry, Department of Materials Sciences, National University of Singapore. The authors wish to thank Dr. Pramoda Kumari, Institute of Materials Research and Engineering (IMRE), for assistance in recording the ATR-FTIR spectra.

References

(1) Wang, B.; Wilkes, G. L. *J. Macromol. Sci. Pure Appl. Chem.* **1994**, *A31*, 249−260.
(2) Calvert, P.; Rieke, P. *Chem. Mater.* **1996**, *8*, 1715−1727.
(3) Reimschussel, H. K. *Handbook of Fiber Chemistry*; Lewin, M., Pearce E. M., Eds.; Marcel Dekker Inc.: New York, 1998; p 84.
(4) Dujardin, E.; Mann, S. *Adv. Eng. Mater.* **2002**, *4*, 461−474.
(5) Yu, Y. Y.; Chen, C. Y.; Chen, W. C. *Polymer* **2003**, *44*, 593−601.
(6) Gower, L. A.; Tirrel, D. A. *J. Cryst. Growth* **1998**, *191*, 153−160.
(7) Lowenstam, H. A.; Weiner, S. *On Biomineralization*; Oxford University Press: New York, 1989.
(8) Mann, S.; Web, J.; Williams, R. J. P., Eds.; *Biomineralization: Chemical and Biochemical Perspectives*; VCH: Weinheim, 1989.
(9) Weiner, S.; Traub, W. *Trans. R. Soc. London* **1984**, *B304*, 425−434.
(10) Belcher, A. M.; Wu, X. H.; Christensen, R. J.; Hansma, P. K.; Stucky, G. D.; Morse, D. E. *Nature* **1996**, *381*, 56−58.
(11) Addadi, L.; Weiner, S. *Nature* **1997**, *389*, 912−913.
(12) Bedouet, L.; Schuller, M. J.; Marin, F.; Milet, C.; Lopez, E.; Giraud, M. *Comp. Biochem. Phys.* **2001**, *B128*, 389−400.
(13) Levi-Kalisman, Y.; Falini, G.; Addadi, L.; Weiner, S. *J. Struct. Biol.* **2001**, *135*, 8−17.
(14) Tong, H.; Hu, J. M.; Ma, W. T.; Zhong, G. R.; Yao, S. N.; Cao, N. X. *Biomaterials* **2002**, *23*, 2593−2598.
(15) Currey, J. D. *Proc. R. Soc. London* **1997**, *196*, 443−463.
(16) Weiner, S. *Crit. Rev. Biochem.* **1986**, *20*, 365−408.
(17) Heywood, B. R. *Microsc. Res. Tech.* **1994**, *27*, 376−388.
(18) Heywood, B. R.; Mann, S. *Adv. Mater.* **1994**, *6*, 9−20.
(19) Donners, J. J. J. M.; Heywood, B. R.; Meijer, E. W.; Nolte, R. J. M.; Sommerdijk, N. A. J. M. *Chem-Eur. J.* **2002**, *8*, 2561−2567.
(20) Kato, T.; Sugawara, A.; Hosoda, N. *Adv. Mater.* **2002**, *14*, 869−877.
(21) Kato, T. *Adv. Mater.* **2000**, *12*, 1543−1546.
(22) Hosoda, N.; Kato, T. *Chem. Mater.* **2001**, *13*, 688−693.
(23) Kato, T.; Suzuki, T.; Amamiya, T.; Irie, T.; Komiyama, N. *Supramol. Sci.* **1998**, *5*, 411−415.
(24) Xu, G. F.; Aksay, I. A.; Groves, J. T. *J. Am. Chem. Soc.* **2001**, *123*, 2196−2203.
(25) Xu, G. F.; Yao, N.; Aksay, I. A.; Groves, J. T. *J. Am. Chem. Soc.* **1998**, *120*, 11977−11985.
(26) Lahiri, J.; Xu, G. F.; Dabbs, D. M.; Yao, N.; Aksay, I. A.; Groves, J. T. *J. Am. Chem. Soc.* **1997**, *119*, 5449−5450.
(27) Aizenberg, J.; Black, A. J.; Whitesides, G. M. *Nature* **1999**, *398*, 495−498.
(28) Aizenberg, J.; Black, A. J.; Whitesides, G. M. *J. Am. Chem. Soc.* **1999**, *121*, 4500−4509.
(29) Aizenberg, J. *J Chem. Soc. Dalton Trans.* **2000**, *21*, 3963−3968.
(30) Aizenberg, J.; Muller, D. A.; Grazul, J. L.; Hamann, D. R. *Science* **2003**, *299*, 1205−1208.
(31) Han, Y. J.; Aizenberg, J. *J. Am. Chem. Soc.* **2003**, *125*, 4032−4033.
(32) Hosoda, N.; Sugawara, A.; Kato, T. *Macromolecules* **2003**, *36*, 6449−6452.
(33) Valiyaveettil, S.; Lakshminarayanan, R. *Polym. Mater. Sci. Eng.* **2001**, *84*, 798.
(34) Lakshminarayanan, R.; Valiyaveettil, S.; Loy, G. L. *Cryst. Growth Des.* **2003**, *3*, 953−958.
(35) Griffith, L. *Acta Mater.* **2000**, *48*, 263−277.
(36) Naughton, B. *J. Med.* **1987**, *18*, 219−250.
(37) Chu, C. C.; Tsai, W. C.; Yao, J. Y.; Chiu, Sindy S. *J. Biomed. Mater. Res.* **1987**, *21*, 1281−1300.
(38) Sudo, S.; Fujikawa, T.; Nagakura, T.; Ohkubo, T.; Sakaguchi, K.; Tanaka, M.; Nakashima, K.; Takahashi, T. *Nature* **1997**, *387*, 563−564.
(39) Panheleux, M.; Bain, M.; Fernanez, M. S.; Morales, I.; Gautron, J.; Arias, J. L.; Hincke, M. T.; Nys, Y. *Br. Poult. Sci.* **1999**, *40*, 240−252.
(40) Yang, D.; Qi, L.; Ma, J. *Adv. Mater.* **2002**, *14*, 1543−1546.
(41) Dennis, J. E.; Carrino, D. A.; Yamashita, K.; Caplan, A. I. *Matrix Biol.* **2000**, *19*, 683−692.
(42) Kitano, Y. *Bull. Chem. Soc. Jpn.* **1962**, *35*, 1973−1980.
(43) Kato, T.; Amamiya, T. *Chem. Lett.* **1999**, *3*, 199−200.
(44) Kato, T.; Suzuki, T.; Amamiya, T.; Irie, T.; Komiyama, M. *Supramol. Sci.* **1998**, *5*, 411−415.
(45) Gower, L. B.; Odom, D. J. *J. Cryst. Growth* **2000**, *210*, 719−734.
(46) Addadi, L.; Moradianoldak, J.; Weiner, S. *ACS Symp. Ser.* **1991**, *444*, 13−27.
(47) Falini, G.; Fermani, S.; Gazzano, M.; Ripamonti, A. *Chem-Eur. J.* **1998,** *4*, 1048−1052.
(48) Kielty, C. M.; Hopkinson, I.; Grant, M. E. *Connective Tissue and its Heritable Disorders*; Wiley-Liss: New York, 1993; p 103.
(49) Arias, J. L.; Nakamura, O.; Fernandez, M. S.; Wu, J. J.; Knigge, P.; Eyre, D. R.; Caplan, A. I. *Connect. Tissue Res.* **1997**, *36*, 21−33.

CG034128E